AFRL-RX-WP-TM-2010-4191

COLLABORATIVE RESEARCH AND DEVELOPMENT (CR&D)

Task Order 0050: Molecular Beam Epitaxial Growth Studies for Optimization of Antimonide Based Heterostructures

Heather Haugan

Universal Technology Corporation

MAY 2008
Final Report

AIR FORCE RESEARCH LABORATORY
MATERIALS AND MANUFACTURING DIRECTORATE
WRIGHT-PATTERSON AIR FORCE BASE, OH 45433-7750
AIR FORCE MATERIEL COMMAND
UNITED STATES AIR FORCE

NOTICE AND SIGNATURE PAGE

Using Government drawings, specifications, or other data included in this document for any purpose other than Government procurement does not in any way obligate the U.S. Government. The fact that the Government formulated or supplied the drawings, specifications, or other data does not license the holder or any other person or corporation; or convey any rights or permission to manufacture, use, or sell any patented invention that may relate to them.

This report was cleared for public release by the USAF 88th Air Base Wing (88 ABW) Public Affairs Office (PAO) and is available to the general public, including foreign nationals. Copies may be obtained from the Defense Technical Information Center (DTIC) (http://www.dtic.mil).

AFRL-RX-WP-TM-2010-4191 HAS BEEN REVIEWED AND IS APPROVED FOR PUBLICATION IN ACCORDANCE WITH THE ASSIGNED DISTRIBUTION STATEMENT.

*//Signature//	//Signature//
MARK GROFF Program Manager Business Operations Branch Materials & Manufacturing Directorate	KENNETH A. FEESER Branch Chief Business Operations Branch Materials & Manufacturing Directorate

This report is published in the interest of scientific and technical information exchange, and its publication does not constitute the Government's approval or disapproval of its ideas or findings.

*Disseminated copies will show "//Signature//" stamped or typed above the signature blocks.

REPORT DOCUMENTATION PAGE

Form Approved
OMB No. 0704-0188

1. REPORT DATE *(DD-MM-YY)*	2. REPORT TYPE	3. DATES COVERED *(From - To)*
May 2008	Final	19 May 2006 – 31 January 2008

4. TITLE AND SUBTITLE
COLLABORATIVE RESEARCH AND DEVELOPMENT (CR&D)
Task Order 0050: Molecular Beam Epitaxial Growth Studies for Optimization of Antimonide Based Heterostructures

5a. CONTRACT NUMBER
F33615-03-D-5801-0050

5b. GRANT NUMBER

5c. PROGRAM ELEMENT NUMBER
62102F

6. AUTHOR(S)
Heather Haugan

5d. PROJECT NUMBER
4349

5e. TASK NUMBER
L0

5f. WORK UNIT NUMBER
4349L0VT

7. PERFORMING ORGANIZATION NAME(S) AND ADDRESS(ES)
Universal Technology Corporation
1270 North Fairfield Road
Dayton, OH 45432-2600

8. PERFORMING ORGANIZATION REPORT NUMBER
S-531-050

9. SPONSORING/MONITORING AGENCY NAME(S) AND ADDRESS(ES)
Air Force Research Laboratory
Materials and Manufacturing Directorate
Wright-Patterson Air Force Base, OH 45433-7750
Air Force Materiel Command
United States Air Force

10. SPONSORING/MONITORING AGENCY ACRONYM(S)
AFRL/RXOB

11. SPONSORING/MONITORING AGENCY REPORT NUMBER(S)
AFRL-RX-WP-TM-2010-4191

12. DISTRIBUTION/AVAILABILITY STATEMENT
Approved for public release; distribution unlimited.

13. SUPPLEMENTARY NOTES
PAO Case Number: 88ABW 2010- 1210; Clearance Date: 16 Mar 2010. Report contains color.

14. ABSTRACT
This research in support of the Air Force Research Laboratory Materials and Manufacturing Directorate was conducted from 19 May 2006 through 31 January 2008. This task worked to develop and optimize molecular beam epitaxy of antimonide-based heterostructures for infrared and terahertz sensor applications. It established the growth and processing conditions necessary for smooth and abrupt interfacial layers in the heterostructure and for reduction of material defects. The optimized growth and processing conditions are detailed in the task final report. There is an increasing demand for uncooled mid-infrared detectors for military applications, therefore recent research task was focused on developing reliable uncooled mid-IR detectors using InAs/GaSb superlattice materials. Approximately 200 samples were grown in this task period using in-house molecular beam epitaxy system, and analyzed by several characterization techniques available in-house or corroborated with local universities around the base.

15. SUBJECT TERMS
antimonide-based heterostructures

16. SECURITY CLASSIFICATION OF:			17. LIMITATION OF ABSTRACT:	18. NUMBER OF PAGES	19a. NAME OF RESPONSIBLE PERSON (Monitor)
a. REPORT	b. ABSTRACT	c. THIS PAGE			Mark Groff
Unclassified	Unclassified	Unclassified	SAR	18	19b. TELEPHONE NUMBER *(Include Area Code)* N/A

Standard Form 298 (Rev. 8-98)
Prescribed by ANSI Std. Z39-18

ACKNOWLEDGMENTS

The author thanks Dr. Frank Szmulowicz of the University of Dayton research institute (UDRI) for theoretical calculation of mid-infrared superlattice designs, Steve. Fenstermaker of UDRI for technical assistance with the MBE system, Mr. Larry Grazulis of UDRI for atomic force microscopy analysis, Dr. Krishnamurthy Mahalingam of Universal Technology Corporation (UTC) and Jared Shank of Southwestern Ohio Council of Higher Education (SOCHE) for transmission electron microscopy (TEM) analysis and sample preparation respectively, Dr. Bruno Ullrich from Bowling Green State University and Lt. Shyam Munshi of AFRL for photoluminescence analysis, and Dr. Said Elhamri from University of Dayton, Mr. Gerry Landis of UDRI, and J. Daniel for Hall analysis and assistance with samples for the Hall measurements, Dr. William Mitchel of AFRL for the helpful discussion with Hall data. In addition, the author thanks Ms. Shanee Houston of AFRL for the assistance of photoresponse measurements and special thank to Dr. Gail Brown of AFRL for general discussion about the program, constant encouragement and photoresponse measurements. This work was supported by the Air Force Office of Scientific Research (AFOSR/NE) through Dr. Don Silversmith and AFRL through Chris Ristich.

1.0 INTRODUCTION

The development of advanced mid-infrared (IR) detectors that can operate at room temperature has gained much attention recently due to increasing demand in thermal imaging, pollutant detection etc.[1-3] Commercially available uncooled IR cameras using focal plane arrays based on thermal detectors are known for low detectivity, slow integration time and small array format.[3] The need for affordable sensors with higher resolution and larger array size is challenging current IR sensor community to explore alternative material systems. Recently, several groups reported prototype *p-i-n* diode arrays using InAs/GaSb superlattices (SLs),[4,5] opening possibilities of their use as uncooled mid-IR sensors.

However, room temperature operation of SLs as minority carrier devices in the *p-i-n* configuration requires a sufficient quantum efficiencies (η) and differential resistances at zero bias (R_oA). Quantum efficiency is determined by the absorption of SL and the minority carrier diffusion length, while R_oA is limited by the dark current resulting mostly from Auger and defect-driven recombination processes.[1,6] For the mid-IR detection (3-5 μm), SLs have achieved reasonably good absorption (~2000 cm^{-1}) due to the intrinsically large electron-hole wave function overlap. Therefore, major objective during growth optimization process is controlling residual background carrier concentrations in unintentionally doped regions of *p-i-n* diodes to increase the minority carrier lifetimes and reduce the dark current.

According to Kinch,[7] residual doping concentrations must be reduced below 10^{14} cm^{-3} in order to produce depletion region widths on the order of 5 μm, which are necessary to achieve sufficient η for room temperature operation. Recently, several papers addressed the issue of lowering the residual carrier doping concentrations,[8-10] however have not reached the desired goal. In particular study of longer wavelength SLs, Bürkle et al.[10] showed the importance of growth temperature (T_g) on the intrinsic carrier type and doping concentration. Moreover, T_g controls anion exchange mechanism that affect interfacial roughness between the layers, which in turn determines both the majority and minority carrier transport properties along the in-plane and growth direction.[10, 11]

In this task period, we optimized several molecular beam epitaxy (MBE) growth parameters, especially growth temperature, to reduce the residual background carrier doping in typical mid-IR 7 ML InAs/8 ML GaSb SLs. In photovoltaic devices, device speed strongly depends on the minority carrier transport and the carrier transport is mainly limited by extrinsic scattering mechanism such as interface roughness scattering (IRS) especially for thin SLs, adjusting growth parameters to reduce interface/layer roughness is important to enhance carrier mobility. Although interface stoichiometry such as the degree of roughness and intermixing can be quantified by few micro-techniques such as scanning tunneling microscopy (STM),[12] it is not realistic to rely on these techniques to be used in routine base to optimize interface quality. Therefore, we used in-plane carrier mobility as an indirect assessment of the quality of SL layers and the degree of IRS. Three growth parameters; growth temperature, in-situ post anneal and interface control were adjusted for the higher in-plane mobility and smoother interfaces. Temperature dependent resistivity and single field Hall measurement was used to monitor intrinsic characteristic of residual carriers in SLs such as the types of carriers, densities and their in-plane mobilities.

2.0 SUPERLATTICE GROWTH

The InAs/GaSb SLs were grown by molecular beam epitaxy on unintentionally doped (100) GaSb (residual *p*-type). Each sample contains a 0.5 μm-thick GaSb buffer layer and a 0.5 μm-thick SL consisting of 110 repeats of alternating 7 ML InAs and 8 ML GaSb layers, which provides the cut-off wavelength around 4 μm in routine base. The V/III beam flux ratio was fixed at ~3, which previously produced smooth surface mopologies.[13] Growth rates of 0.9 Å/s and 0.25 Å/s are used to grow the intended InAs and GaSb layers, respectively. Detail growth conditions have been reported elsewhere.[13] The structural parameters such as strain and the SL period were determined by high resolution x-ray rocking curves (HRXRC), and the measured period of 45 Å±0.3 Å was very close to the intended value. The band gap of the design was determined by photoresponse and photoluminescence measurements.

3.0 RESULTS AND DISCUSSIONS

To determine residual carrier properties, conventional variable temperature Hall effect measurements were performed on each grown sample. Ohmic contacts were placed at the corners of roughly 1x1 cm^2 van der Pauw samples, and variable temperature (10-300 K) resistivity and single field (0.5 T) Hall measurements were performed in a guarded direct-current system. Because residual p-type GaSb substrates can show significant conduction throughout the temperature range (10-300 K), the Hall mobilities (μ) from SL samples were compared with those obtained from a typical GaSb substrate (Fig. 1).

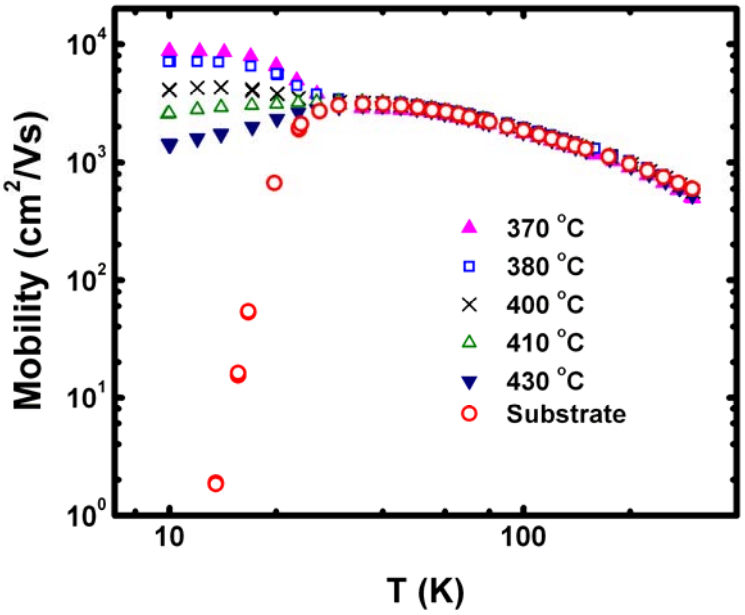

Figure 1. The in-plane carrier mobility as a function of growth temperature for the 7 ML InAs/8 ML GaSb superlattices (SLs) grown between 370 to 430 °C and the GaSb substrate. Below 20 K, substrate conduction is frozen out so that the 10 K mobility is dominated by SL themselves.

Above 20 K, the mobility is dominated by the parallel conduction channel through the p-type substrate. Blow 20 K, the SL and substrate present competing parallel conduction channels as the number of mobile holes in the substrate increases. Below 10 K, holes in the substrate move only via hopping with negligible mobilities. Therefore, we take the 10 K results as the characteristic of the SL themselves. Figure 2 plots the 10 K-carrier densities as a function of T_g. The lowest carrier density of 1.8 $x10^{11}$ cm^{-2} (~3.6 $x10^{15}$ cm^{-3}) was obtained from the SL grown at 400 °C. At T_g below or above 400 °C, the carrier density slightly increases at a most a factor of two (3.2 $x10^{11}$ cm^{-2}), but still stays in the low 10^{11} cm^{-2}. All SL samples in the series were residual p-type and remained as p-type throughout the entire temperature range studied (10-300 K).

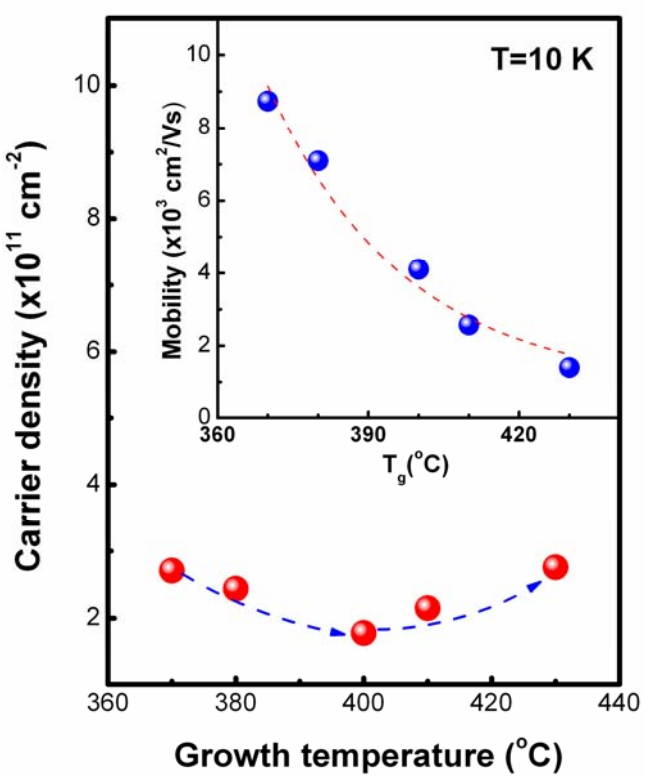

Figure 2. The carrier density and in-plane mobility (the insert) as a function of the growth temperature (T_g) for the 7 ML InAs/8 ML GaSb superlattice measured at 10 K.

This differs from the results of an earlier magnetic transport study done on longer wavelength 10 ML InAs/5 ML $In_{0.25}Ga_{0.75}Sb$ (binary/ternary) systems.[10] The SLs grown at 360 and 380 °C were residual n-type with electron concentration as high as the low 10^{16} cm^{-3}, meanwhile those grown at 400, 420, and 440 °C were residual p-type with hole concentration maximum as high as the high 10^{15} cm^{-3}. In our experience, InAs normally grows n-type and GaSb p-type, therefore the difference seen in Ref. 10 might be coming from using different ratios of the GaSb-to-InAs layer widths; for our SLs, the ratio is 8-to-7 that favors p-type SLs, whereas the ratio in Ref. 10 is 1-to-2 that favors n-type SLs as observed. The behavior seen in Fig. 2 can be explained using similar arguments claimed in Bürkle et al.[10] Lower T_g lead to an excess of group V elements, which leads to group III vacancies. Increased incorporation of residual group IV impurities at vacant group III sites, where they act as donors, causes the SLs to be less p-type as seen in Fig. 2 from 370 to 400 °C. With increasing T_g, the excess of group V atoms decreases, the number of group III vacancies decreases, so that the residual group IV impurities begin to incorporate at group V sites, where they act as acceptors. The overall trend is to make the SLs more p-type, as seen in Fig. 2 above 400 °C. However, the residual carrier density in Ref. 10 changes by about an order of magnitude, whereas the variation in Fig. 2 is only by about a factor of two. The latter observation is consistent with the fact that our SLs are p-type to begin with.

In photovoltaic devices, efficient minority carrier conduction and diffusion require high carrier mobilities for higher speeds of operation and greater diffusion lengths. Since the mobilities of minority and majority carriers in the growth and in-plane directions are mainly

limited by interface roughness scattering (IRS),[11] we can take the in-plane majority carrier mobilities to be indicative of the minority carrier mobilities in the growth direction as well as of the sample quality itself.[11] The insert of Fig. 2 shows the 10 K in-plane majority hole mobility as a function of T_g. As the T_g increases from 370 to 430 °C, the in-plane hole mobilities decrease six fold. In our previous mobility study of the n-type SLs with increasing InAs layer width,[11] the mobilities were IRS-limited as evidenced by the temperature independence of their mobilities around 10 K and their classic sixth-power dependence on layer widths. Because hole masses in the growth direction are an order of magnitude greater than the electron mass, holes are better confined in the GaSb layers than are electrons in the InAs layers. Hence, holes should be more sensitive to interface roughness fluctuations than are the more itinerant electrons. The degree of interface roughness can be extracted based on the available models,[14] according to which mobility μ is given by

$$\mu = \frac{eL^6}{\pi^5 \hbar \Delta^2 \Lambda^2} \times F\left(\Lambda, k_F\right)^{-1},$$

where Δ is the interface roughness, Λ the coherence length of interface fluctuations, L the width of the current-carrying layer, k_F the Fermi wave vector, and $F\left(\Lambda, k_F\right)$ is a scattering integral that depends on screening. Using $k_F^{-1} \approx 890$ Å and the calculated screening length of $q_s^{-1} \approx 100$ Å, we find $F(\Lambda, k_F) \approx 0.010$, so that $\mu \approx \left(1.04 \times 10^7 cm^2/V \sec\right)/(\delta\lambda)^2$, where λ and δ are the numerical values of Λ and Δ in Å. With 1 ML roughness, $\delta = 3.048$, so that $\Lambda = 12$ Å at 370 K and $\Lambda =$ 28 Å at 420 K; for 2 ML roughness, $\delta = 6.096$, and the Λ numbers are halved. Therefore, for 1 to 2 ML roughness, Λ is on the order of 10-30 Å, which agrees with our estimates on n-type SLs for mid-IR detection.[15] Overall, the mobility decrease can be ascribed to the increase of either Λ or Δ.

In addition, photoluminescence (PL) measurements were used to evaluate the optical quality of the SLs and to establish a correlation between the observed electrical properties and optical quality. The PL peak corresponds to the band gap recombination of photoexcited minority carriers (here, electrons) in the InAs layer with residual holes in the GaSb layer, which makes the PL intensity sensitive to the electron-hole wave function overlap as well as to the presence of any nonradiative recombination processes. The PL measurements were performed by exciting the sample with a diode pumped Neodymium Vanadate (Nd:YVO4) laser at 532 nm. The sample was placed in an optical Janis cryostat and the emitted PL intensity was detected with a nitrogen cooled InSb detector. Figure 3 shows three representative luminescence spectra with absolute intensities collected from the SLs grown at 380, 400, and 420 °C. For all SLs in the series, the peak energy and the full width at half maximum (FWHM) are around 300-305 meV and 6-7 meV regardless of T_g. Since the peak position remains constant, the confinement potential for the carriers is independent of the T_g, from which we infer that the interface abruptness characterized by Δ does not change. This is further corroborated by the invariance of the FWHM of the spectra in Fig. 3. By contrast, the PL spectra in Bürkle's study[10] show a pronounced red shift of 11 meV, which they attributed to the reduced abruptness of their SLs through interface inter-diffusion involving anion interchange. Our findings suggest that the behavior of the mobility in the insert of Fig. 2 is due to the increase in the correlation length Λ rather than in the height Δ of interface fluctuations.

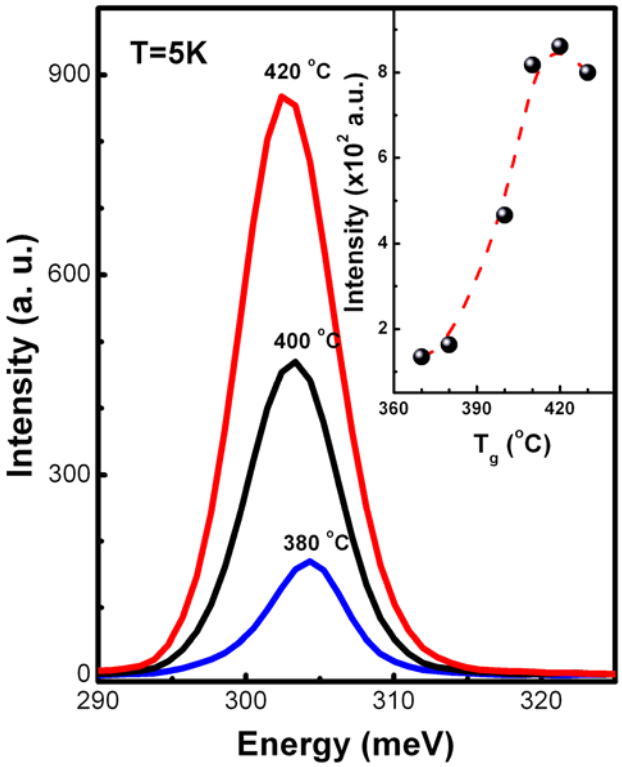

Figure 3. The 5 K photoluminescence spectra of three 7 ML InAs/8 ML GaSb superlattices grown at 380, 410 and 420 °C, respectively. The inset shows the PL intensity as a function of growth temperature.

The insert of Fig. 3 plots the 5 K PL intensity as a function of T_g showing four fold increases in intensity as T_g increases from 370 to 400 °C, and reaching the maximum at 410 and leveling off, which is similar to the behavior observed in Ref. 10. Bürkle et al. used different mechanisms to explain the PL behavior in their n- and p-type samples. In their p-type samples, the intensities saturate, which is explained by the nonradiative recombination of minority electrons that diffuse to the SL surface. Since such recombination is independent of hole concentration, the PL intensity is independent of T_g. In our case, the diffusion length $L_n = \sqrt{k_B T \mu_n \tau_n / e}$, so with the electron mobility $\mu_n = 3{,}000$ cm^2/Vsec, $T = 10$ K, and the minority carrier lifetime $\tau_n = 10^{-9}$ sec,[16] we find $L_n = 5000$ Å, which is on the order of the SL thickness, consistent with the mechanism explained above. For our p-type samples, we explain the initial fast rise in the PL intensity by a rapid decrease in the number of nonradiative recombination centers such as vacancies in the SL itself, which agrees with the behavior of the carrier concentration data in Fig. 2. As the samples become more p-type, the PL intensity is also enhanced by the increase in the number of holes for electrons to recombine with. Then, as nonradiative defects are reduced, surface recombination becomes the rate limiting step and the PL intensities saturate.

In minority carrier devices, device performance relies on the carrier transport, therefore we studied two other growth parameters; in-situ post annealing and interface control to improve carrier mobilities and interface/layer quality. For annealing study, four SLs were grown at 400 °C, and three SLs were annealed in-situ at 450, 475 and 490 °C for 15 minutes under Sb-over

pressure immediately after SL growth. Carrier density and in-plane mobility of annealed samples were then compared to those of the unannealed sample in figure 4.

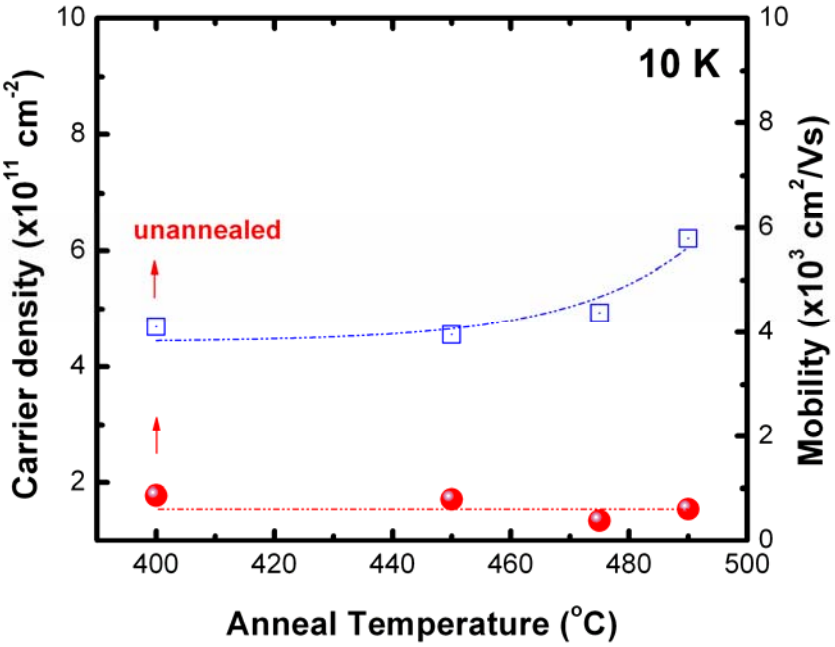

Figure 4. The carrier density (●) and in-plane mobility ( ) of annealed superlattices comparing with those of unannealed superlattices.

For the carrier density, we observed no significant difference between un-annealed and annealed samples, all of which showed a density around 1.6×10^{11} cm^{-2}. For the majority carrier mobilities, in-situ annealing improves the mobility slightly, especially at higher annealing temperatures (above 450 °C), but the factor of 1.5 is not considered significant. All annealed SLs in this set were residual p-type as well.

Another growth parameter studied to improve interfacial quality was interface control. In InAs/GaSb SLs grown on GaSb substrates, InAs will be in tension and adjusting the interface shutter sequences to relieve this tension is required to grow thicker and dislocation free structures. Much effort has been devoted to controlling the interface to produce smoother interfaces. Without intentional interface control in our GaSbInAsGaSb…growth sequence, InSb-like interfacial bonds naturally form for InAs-on-GaSb, while GaAs-like bonds are likely for GaSb-on-InAs, resulting in -0.13 % strain (tension), which is measured by HRXRC. As a systematic approach to study the effect of interface shutter sequence on the strain and interfacial quality, four variations of interface shutter sequences were investigated, noted as; InSb/GaAs, InSb/InSb, GaAs/GaAs, and GaAs/InSb. The interface formation order was written from the left to the right. For example, to form the InSb/GaAs interface sequence; immediately after GaSb layer growth, the Ga shutter was closed while Sb-flux continued for 1 second and 0.3 Å of indium (1 s) was then deposited without Sb-flux and then InAs layer growth was continued. After InAs layer growth, the In shutter was closed while As-flux continued for 1 s and then 0.3 Å of gallium (0.5 s) was deposited without As-flux and continued GaSb layer growth. The amounts of interface mentioned here are estimated values from shutter sequence time, and more practically, will be mixed quaternary alloys of $In_xGa_{1-x}Sb_yAs_{1-y}$. All SLs in this set were grown at 400 °C, the measured structural and electrical parameters were summarized in Table 1. The

table shows that measured periods of all five SLs were around 45 Å as intended, however the strain and in-plane mobility were very sensitive to the interface shutter sequences. Since InSb-like (GaAs-like) interface would relieve tension (compression), the combination of both types of interfaces can be used profitably to balance strain in the SLs. For our series, by inserting two InSb (GaAs)-like interfaces, the -0.13 % of strain was able to be relieved to +0.10 % (-0.3 %). The strain values with different combination of interface types can be found in Table 1.

Table 1. Data summary of 21 Å (InAs+IF)/24 Å (GaSb+IF) superlattices. The 0.3 Å of InSb-like or/and GaAs-like interfaces (IF) were inserted between the layers and their values were estimated from shutter time. The 0/0 represents uncontrolled interface. The R_s, n_s and μ represent resistivity, hole density and in-plane hole mobility.

Interface type	Period Å	Strain %	R_s Ω/sq	n_s $x10^{11}$ cm^{-2}	μ cm^2/Vs
0/0	44.8	-0.13	8563	1.8	4104
InSb/GaAs	45.4	-0.08	3412	2.8	6600
InSb/InSb	45.5	+0.10	7000	2.0	4355
GaAs/GaAs	45.2	-0.30	7682	1.5	5500
GaAs/InSb	45.1	-0.15	42000	58	26

For the interface abruptness, among the four interface types described in Table 1, the InSb/GaAs is the most desirable (expected to be formed the smoothest interface) and the GaAs/InSb the least desirable (the roughest) interface sequence, because it is the former that promotes natural interfacial bonds on both sides. This demonstrated from the result shown in Table 1, where we observe a drastic reduction in the in-plane mobility of the GaAs/InSb interface sequence (26 cm^2/Vs) whereas the others show a moderate improvement in comparison to the uncontrolled sequence 0/0 (4100 cm^2/Vs). With the GaAs/InSb interface sequence, the carrier doping density increased from the low 10^{11} cm^{-2} range to $6x10^{12}$ cm^{-2}, demonstrating the sensitivity of interface shutter sequence on the quality of layers/interfaces, and thus carrier doping and mobility. Figure 5 summarizes the effect of different interface shutter sequences on carrier properties. All SLs with controlled interfaces were residual p-type.

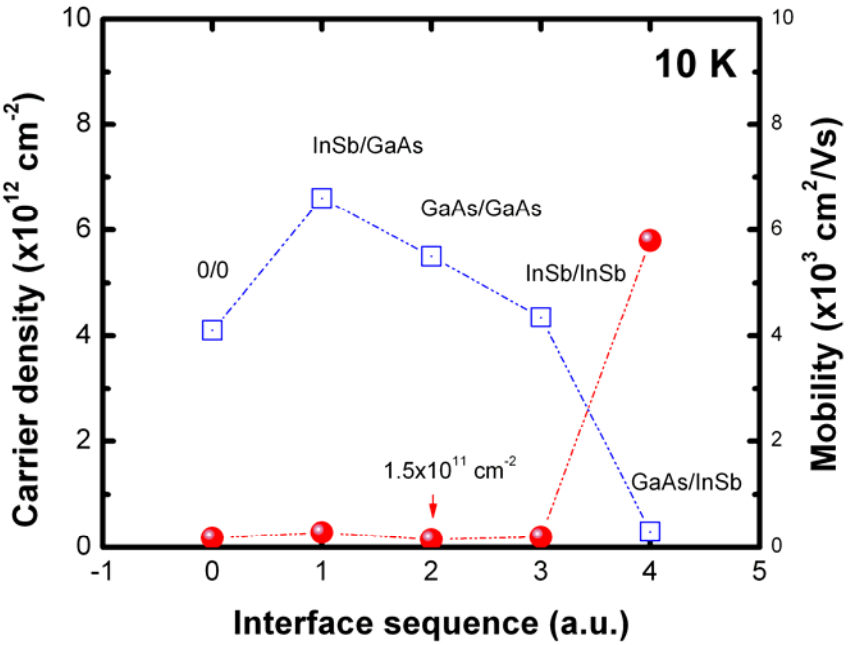

Figure 5. The carrier density and in-plane mobility of the 21 (InAs+IF)/24 (GaSb+IF) superlattices with four variations of interface shutter sequences. The 0/0 represents uncontrolled sequence.

4.0 CONCLUSIONS

Several SL growth parameters were tuned for the lower carrier doping density and higher mobility in a typical mid-infrared 21 Å InAs/24 Å GaSb SLs. Over the 370-430 °C growth temperature (T_g) range studied, the lowest doping density of $1.7x10^{11}$ cm^{-2} was achieved at 400 °C and overall residual density remained in low 10^{11} cm^{-2} even with large differences in growth temperatures. With increasing T_g, however, in-plane carrier mobility decreased from 8740 to 1400 cm^2/Vs. Overall carrier density from all SLs grown at 400 °C remained around $1.6x10^{11}$ cm^{-2} with or without in-situ post annealing and in-plane carrier mobility showed slight improvement with annealing especially at higher annealing temperatures of 475 °C and above. We demonstrated in-plane carrier mobility could be used as an indirect assessment of interface/layer quality. With improper interface shutter sequence, doping densities increased from ~$2x10^{11}$ to ~$6x10^{12}$ cm^{-2} and simultaneously carrier mobilities dropped from 6600 to 26 cm^2/Vs. All SLs studied in the paper were residually p-type.

REFERENCES

[1]A. Rogalski, Infrared Phys. Technol. **50**, 240 (2007).

[3]L. Becker, Proc. SPIE. **6127**, 61270S (2006).

[3]T. Ashley, N. T. Gordon, Proc. SPIE. **5359**, 89 (2004).

[4]M. Razeghi, Y. Wei, A. Hood, D. Hoffman, B. M. Nguyen, P. Y. Delaunay, E. Michel, R. McClintock, Proc. SPIE. **6206**, 62060N (2006).

[5]M. Walther, J. Schmitz, R. Rehm, S. Kopta, F. Fuchs, J. Fleiner, W. Cabanski, J. Ziegler, J. Cryst. Growth **278**, 156 (2005); M. Walther, G. Weimann, Phys. Stat. Sol. (a) **203**, 3545 (2006).

[6]J. Piotrowski and A. Rogalski, Proc. SPIE. **5359**, 10 (2004).

[7]M. Kinch, Proc. SPIE. **4454**, 168 (2001); M. Kinch, Proc. SPIE. **4288**, 254 (2001).

[8]A. Hood, D. Hoffman, Y. Wei, F. Fuchs, M. Razeghi, Appl. Phys. Lett. **88**, 052112-1 (2006).

[9]E. Silva, D. Hoffman, A. Hood, B. M. Nguyen, P. Y. Delaunay, M. Razeghi, Appl. Phys. Lett. **89**, 243517 (2006).

[10]L. Bürkle, F. Fuchs, J. Schmitz, W. Pletschen, Appl. Phys. Lett. **77**, 1659 (2000).

[11]F. Szmulowicz, S. Elhamri, H. J. Haugan, G. J. Brown, W. C. Mitchel, J. Appl. Phys. **101**, 043706-1 (2007).

[12]B. Z. Nosho, W. Barvosa-Carter, M. J. Yang, B. R. Bennett, L. J. Whitman, Surf. Science **465**, 361 (2000).

[13]H. J. Haugan, L. Grazulis, G. J. Brown, K. Mahalingam, D. H. Tomich, J. Cryst. Growth **261**, 471 (2004); H. J. Haugan, K. Mahalingam, G. J. Brown, W. C. Mitchel, B. Ullrich, L. Grazulis, S. Elhamri, J. C. Wickett, D. W. Stokes, J. Appl. Phys. **100**, 123110 (2006).

[14]A. Gold, Phys. Rev. B **35**, 723 (1987).

[15]F. Szmulowicz, S. Elhamri, H. J. Haugan, G. J. Brown, W. C. Mitchel, to be published in Proc. SPIE. 2008.

[16]Jian V. Li , Shun Lien Chuang, Eric M. Jackson, Edward Aifer, Appl. Phys. Lett. **85**, 1984 (2004); E. R. Youngdale, J. R. Meyer, C. A. Hoffman, F. J. Bartoli, C. H. Grein, P. M. Young , H. Ehrenreich, R. H. Miles, D. H. Chow, Appl. Phys. Lett. **64**, 3160 (1994).